Journal of the Iranian Chemical Society (2019) 16:1563–1570
https://doi.org/10.1007/s13738-019-01629-y

ORIGINAL PAPER

Synthesis of magnetite-supported catalysts for phenol oxidation in aqueous solution

M. Rezaie[1] · **M. Anbia**[1]

Received: 20 September 2018 / Accepted: 2 February 2019 / Published online: 21 February 2019

Abstract
One of the usual ways to degrade phenol contaminant is sulfate radical-based advanced oxidation processes (SR-AOPs). In this study, reactive sulfate radicals have been produced by $Co_3O_4/Fe_3O_4@nSiO_2@mSiO_2$ catalyst and Fe_3O_4 nanoparticles. It has been found that the couple of supported cobalt catalyst and peroxymonosulfate (PMS) is highly effective to produce sulfate radicals for phenol oxidation. In contrary to, Fe_3O_4-PMS system displays much low phenol degradation, and $Co_3O_4/Fe_3O_4@nSiO_2@mSiO_2$ catalyst shows a good catalytic performance in solution. The properties of this supported catalyst have been characterized by XRD (powder X-ray diffraction), SEM–EDS (scanning electron microscopy–energy-dispersive X-ray spectroscopy), TEM (transmission electron microscopy), and nitrogen adsorption–desorption. This magnetic catalyst is facility separated from the medium by an external magnetic field. Finally, three different methods involving annealing in the air, washing with water and applying ultrasonics was used for regenerating the deactivated catalyst. The heat treatment can recover the catalyst nearly.

Keywords $Co_3O_4/Fe_3O_4@nSiO_2@mSiO_2$ mesoporous catalyst · Peroxymonosulfate (PMS) · Advanced oxidation processes (AOPs) · Phenol degradation · Magnetic separation

Introduction

The presence of phenol and its derivatives in water has become a main water pollutants which have toxic effects on the environment even at low concentrations. The phenolic contaminants are byproducts of several industries such as petrochemical, petroleum refining, pharmaceutical, plastic, and pesticide industries [1, 2]. The technique such as primary and secondary treatment methods cannot easily remove these organic contaminants. Hence, it is essential to adopt a tertiary treatment such as wet air oxidation, thermal oxidation, chemical oxidation, catalytic oxidation, etc., that are generally known as advanced oxidation processes (AOPs) [3–10]. These methods, which involve highly reactive oxidizing species such as hydroxyl radical and sulfate radical, have attracted great interests in the areas of water treatment [10–13].

In principle, the AOPs will produce compounds harmless to the environment such as CO_2 and H_2O. Hydroxyl radicals have been widely applied in various chemical processes due to their remarkable reactivity towards many organic reactants. However, these radicals suffer from many limitations, such as complicated radical generation processes, pH-tuning, and potential sludge generation [14, 15]. Recently, utilization of sulfate radicals instead of hydroxyl radicals in oxidation processes has been widely carried out due to its higher selectivity and reactivity as a result of its superior characteristics in comparison with hydroxyl radicals [16]. In the previous investigations, the reaction of cobalt ion and peroxymonosulfate (PMS) for sulfate radical production provides an impressive method for oxidation of organic contaminants in water [14, 17–21]. However, the main problem in using cobalt ions as catalysts to activate PMS is the toxicity of this heavy metal in the treatment system. These metal ions can cause several health problems such as asthma and pneumonia [20, 22]. Therefore, to prevent cobalt discharging in wastewater, development of heterogeneous catalysts is required. For this purpose, the transition metals should be loaded into solid supports such as silica, alumina, and zeolite. Heterogeneous catalysts have been applied for many chemical and

✉ M. Anbia
anbia@iust.ac.ir

[1] Research Laboratory of Nanoporous Materials, Faculty of Chemistry, Iran University of Science and Technology, Farjam Street, 16846-13114 Narmak, Tehran, Iran

photochemicals reactions [23–25] and can be easily mineralize, and organic compounds undergo reactions. They can be completely convert to CO_2 and H_2O or moderately oxidize the organic compounds to less toxic ones [26, 27]. The selection of suitable supports is vital in the preparation of Co-based catalysts and their applications. Mesoporous silica materials have different applications, and in water treatment processes, they are the best option as adsorbent and catalyst, due to their large surface area, high mechanical strength, nontoxicity, and thermal and chemical stability [28].

When the volume of catalytic solution is high, the separation of catalyst from medium is time-consuming, so the use of superparamagnetic materials for catalytic applications has been developed [29]. These materials can easily be retrieved by a magnetic field and reused.

In this paper, to prepare a cobalt-based catalyst, a new core–shell microsphere with a magnetic core, a middle nonporous silica shell, and an outer cobalt-functionalized mesoporous silica shell have been synthesized. This supported catalyst has demonstrated high magnetic efficiency and activity in oxidation of phenol solution.

Materials and methods

Chemicals

All chemical substances employed were of analytical grade. Furthermore, deionized water was utilized to prepare the solutions.

Preparation of Fe_3O_4

Magnetite was prepared by a co-precipitation method. In the beginning of the reaction, 5 g $FeCl_3{\cdot}6H_2O$ and 2 g $FeCl_2{\cdot}4H_2O$ were dissolved in deionized water under constant stirring. Afterward, NaOH solution [30% (w/v)] was added dropwise with nitrogen bubbling, so that the pH reached 10 and Fe_3O_4 nanoparticles were synthesized. The suspension was stirred constantly for 30 min, and then, the vessel was transferred to an oil bath to be heated at 90 °C for 1 h. Finally, the black nanoparticles were cooled down to room temperature, and then, the resultant product was washed with a mixture of ethanol/water for several times and dried at 60 °C overnight.

Preparation of Fe_3O_4@nSiO_2@mSiO_2

A typical hydrolysis reaction was applied for synthesis of Fe_3O_4/silica spheres. In the beginning, 2 g magnetic particles were washed by 0.1 M HCl solution mixture and then transferred to a solution containing 20 mL H_2O, 80 mL ethanol, and 1 mL of aqueous ammonia (25 wt %). After dispersing this mixture, 1 mL tetraethyl orthosilicate (TEOS) was added dropwise into the solution and stirred vigorously at room temperature for 12 h. After that, the product was divided and washed with ethanol and deionized water and then dispersed for 30 min in a solution containing 80 mL deionized water, 60 mL ethanol, 6 g CTAB, and 1.2 mL of aqueous ammonia (25 wt%). Subsequently, 9 mL of TEOS was added to the above mixture under stirring. After reacting for 12 h, the product was collected with a magnet and washed with ethanol and deionized water. At the last step, surfactant template was removed by dispersing particles in 100 mL ethanol and refluxed at 90 °C for 48 h. Eventually, the obtained solid (Fe_3O_4@nSiO_2@mSiO_2) was dried at 60 °C overnight.

Preparation of Co_3O_4/Fe_3O_4@nSiO_2@mSiO_2 catalyst

In general, an impregnation method was utilized for synthesis of Fe_3O_4@nSiO_2@mSiO_2-supported cobalt oxides. First, a fixed amount of magnetic support was dispersed in 90 mL of ethanol for 15 min, then, $Co(NO_3)_2.6H_2O$ (Sigma–Aldrich) and 50 mL ethanol were added to the mixture and kept stirring intensively for 16 h, and then dried at 60 °C. The resultant material was heated at 200 °C for 2 h and the loading of Co on the support was maintained at 5 wt%.

Characterization

The obtained catalyst was characterized by X-ray diffraction (XRD), nitrogen adsorption–desorption, scanning electron microscopy–energy-dispersive X-ray spectroscopy (SEM–EDS), and transmission electron microscopy (TEM). The structural features and the mineralogy of the support and catalyst were studied by XRD patterns. The spectra were recorded on a Philips 1830 diffractometer with Cu-Kα ($\lambda = 0.154$) radiation at a current of 30 mA and voltage of 30 kV. The chemical compositions and external morphology of the Fe_3O_4 cores were observed using SEM (scanning electron microscopy, Philips XL 30). EDS was also utilized to detect the cobalt particles on the support. The particle structures were determined by TEM (transmission electron microscopy) operated at 100 kV (Zeiss-EM10C). The specific surface area of the catalyst was evaluated by N_2 adsorption–desorption. The support and catalyst were degassed at 120 °C for 12 h prior to the analysis.

Experimental procedure

Catalytic oxidative examinations were performed by degrading 500 mL phenol solution with a concentration of 50 ppm. This mixture was stirred severely in a glass beaker to obtain a homogeneous solution at 25 °C. Subsequent, a fixed amount of catalyst was added to the solution to achieve adsorption–desorption equilibrium. Then, a known amount

of peroxymonosulfate (oxone) as an initial reactant was added to the mixture. The reaction was done for 3 h. During appropriate time interval, 50 mL of the solution was separated and mixed with excess of sodium nitrite as a quenching reagent. Eventually, the magnetic catalyst was separated from the solution using a magnet. Next, phenol concentrations were determined by standard method employed 4-aminoantipyrine at maximum wavelength of phenol, i.e., 500 nm using spectrophotometric measurements (UV/Vis mini 1240 Shimadzu).

Results and discussion

Characterization of cobalt impregnated Fe_3O_4@ $nSiO_2$@$mSiO_2$ catalyst

Figure 1 shows the XRD patterns of support and Co_3O_4/Fe_3O_4@$nSiO_2$@$mSiO_2$. The core–shell materials exhibit diffraction patterns similar to that of Fe_3O_4 microspheres [30], suggesting that the SiO_2 shells were well formed on the magnetic microspheres. Owing to the amorphous nature of silica, we cannot see a sharp peak in XRD pattern of Fe_3O_4@$nSiO_2$@$mSiO_2$, and as can be perceived in Fig. 1b, a diffusive peak at around 2θ 20 present in the patterns of as-prepared core/shell structure, is related to the SiO_2 layer. It can be seen that cobalt species are found in the form of Co_3O_4 on Co_3O_4/Fe_3O_4@$nSiO_2$@$mSiO_2$ in Fig. 1c [31].

Morphology and structure of the synthesized magnetic nanoparticles have been perused by SEM images. Figure 2a shows the sphere-like morphology of Fe_3O_4 core nanoparticles. The EDS measurement illustrates that cobalt has been successfully loaded on the support. Thus, the EDS spectra confirm the XRD results.

The core/shell structure of Fe_3O_4@$nSiO_2$@$mSiO_2$ as support display by TEM image of particles (Fig. 3).

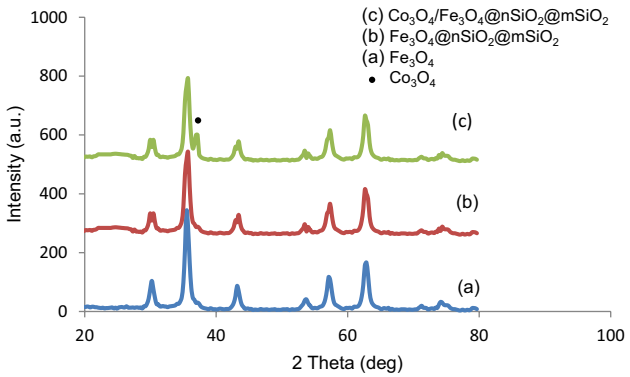

Fig. 1 XRD patterns of Fe_3O_4 **a**, Fe_3O_4@$nSiO_2$@$mSiO_2$ **b**, and Co_3O_4/Fe_3O_4@$nSiO_2$@$mSiO_2$ **c**

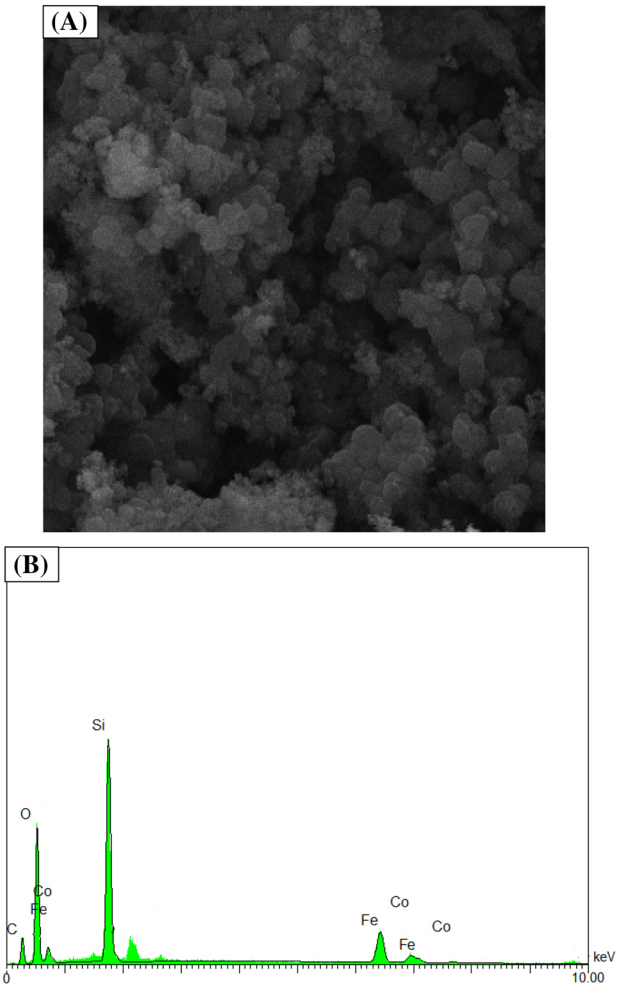

Fig. 2 SEM image of Fe_3O_4 core nanoparticles (**a**) EDS spectra of Co_3O_4/Fe_3O_4@$nSiO_2$@$mSiO_2$ (**b**)

The porous structure of the support and catalyst samples has been determined by N_2 adsorption (Fig. 4). It is found that the BET surface area of Fe_3O_4, Fe_3O_4@$nSiO_2$@$mSiO_2$ and Co_3O_4/Fe_3O_4@$nSiO_2$@$mSiO_2$ was 102, 394, and 316 m^2/g, respectively. This demonstrates that after loading of Co_3O_4 species, the specific surface area of the catalyst became lower than the support. The hysteresis loop suggests a typical mesoporous structure (isotherm Type IV) of Fe_3O_4, support and Co_3O_4/Fe_3O_4@$nSiO_2$@$mSiO_2$ samples.

Adsorption and heterogeneous phenol degradation

Actually, in catalytic oxidation process, various transition metals in the form of oxides can be applied. Indeed, transition metal participates in the redox reactions (Eqs. 1, 2) for generation of sulfate radicals and the redox potential of M^{2+}/M^{3+} will be an important factor. For heterogeneous oxidation of phenol, activation of PMS occurred on the surface of oxide particles [25, 32]:

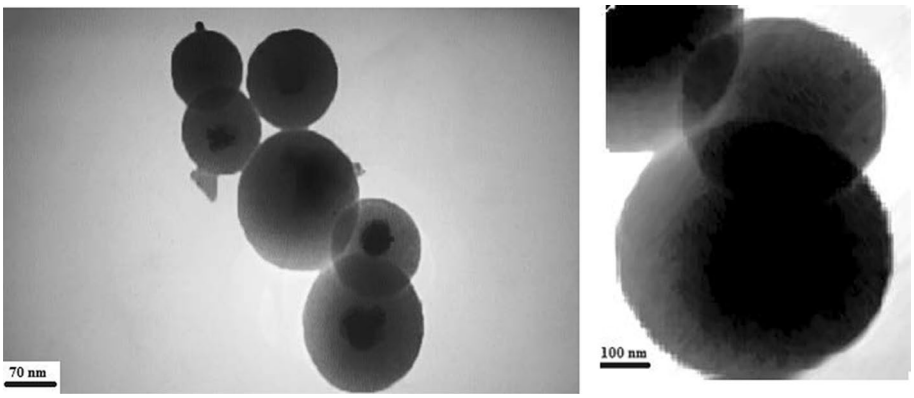

Fig. 3 TEM image of Fe_3O_4@$nSiO_2$@$mSiO_2$ as support

$$HSO_5^- + 2MO \rightarrow SO_4^{\bullet -} + H^+ + M_2O_3 \quad M = Fe, Co, Mn, Ru, \ldots \tag{1}$$

$$HSO_5^- + M_2O_3 \rightarrow SO_5^{\bullet -} + OH^- + 2MO \tag{2}$$

Transition metals such as Co (II) and Ru (III) are the best metal catalysts for the generation of sulfate radicals [32]. The reaction of Co (II) with PMS can be described as the follows:

$$Co\ (II) + HSO_5^- \rightarrow Co\ (III) + OH^- + SO_4^{\bullet -} \tag{3}$$

The following procedures show the steps of phenol oxidation:

$$S\text{-}Co\ (III) + HSO_5^- \rightarrow S\text{-}Co\ (II) + H^+ + SO_5^{\bullet -}\ (S: \text{solid surface}) \tag{4}$$

$$S\text{-}Co\ (II) + HSO_5^- \rightarrow S\text{-}Co\ (III) + OH^- + SO_4^{\bullet -} \tag{5}$$

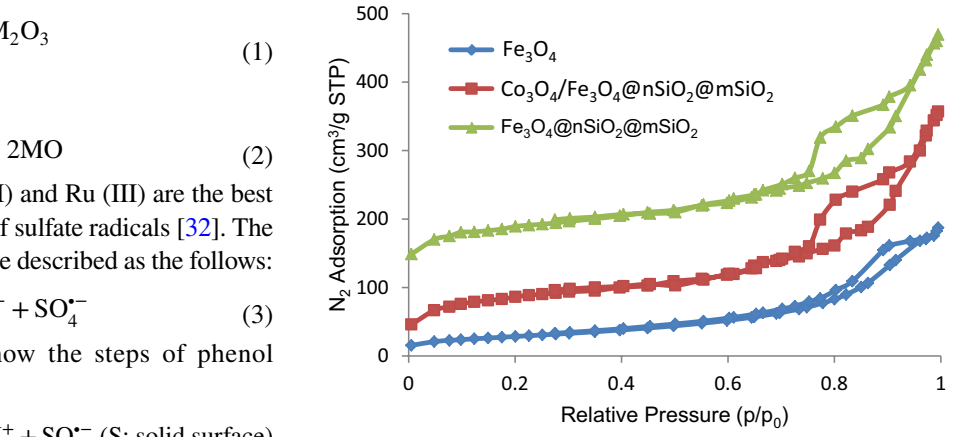

Fig. 4 N_2 adsorption–desorption isotherms of Fe_3O_4, Fe_3O_4@$nSiO_2$@$mSiO_2$ and Co_3O_4/Fe_3O_4@$nSiO_2$@$mSiO_2$

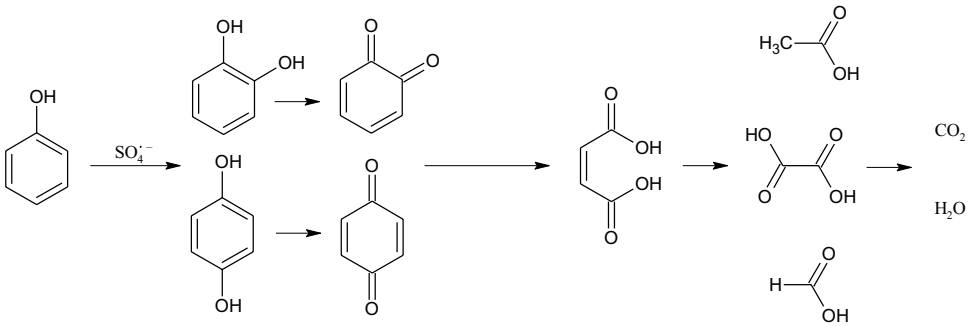

(6)

The original intermediates such as catechol, hydroquinone, benzoquinone, maleic acid, oxalic acid, and acetic acid are produced in the presence of sulfate radicals. The latter intermediates are finally mineralized to CO_2 and H_2O [33–36]. Phenol removal is a fast reaction, and in any experiment, color shows the path of a reaction intermediate, so it might be possible to establish a relationship between the color level observed and the intermediate compounds generated during the oxidation. In the first stages of oxidation, highly colored intermediate compounds such as p-benzoquinone (yellow) and o-benzoquinone (red) are generated. Their color comes from their quinoidal structure, which contains chromophore groups substituted in benzene rings. After a while, colored intermediates start to degrade to colorless compounds. This degradation takes place slowly, because quinone-type compounds seem to be a very stable species in this

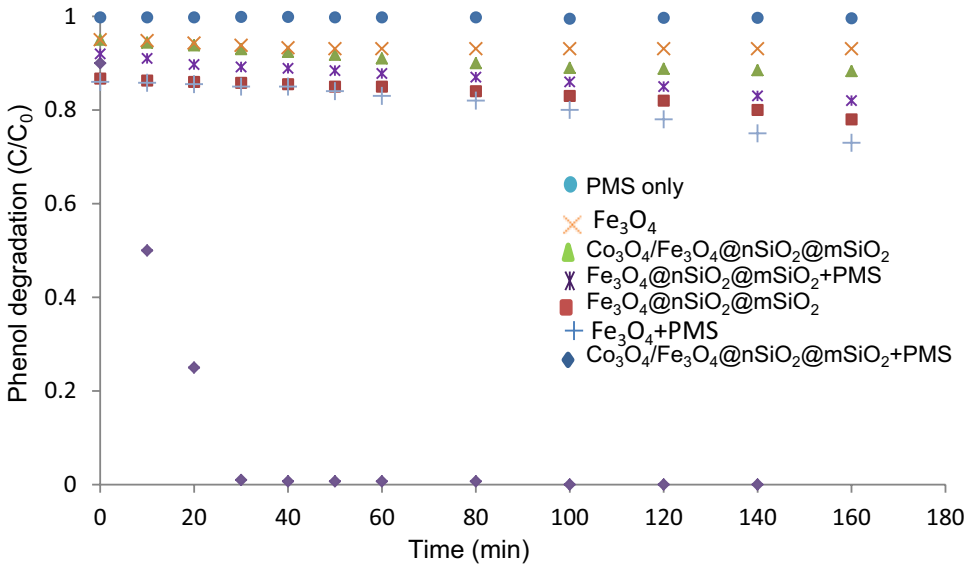

Fig. 5 Phenol removal in various reaction conditions

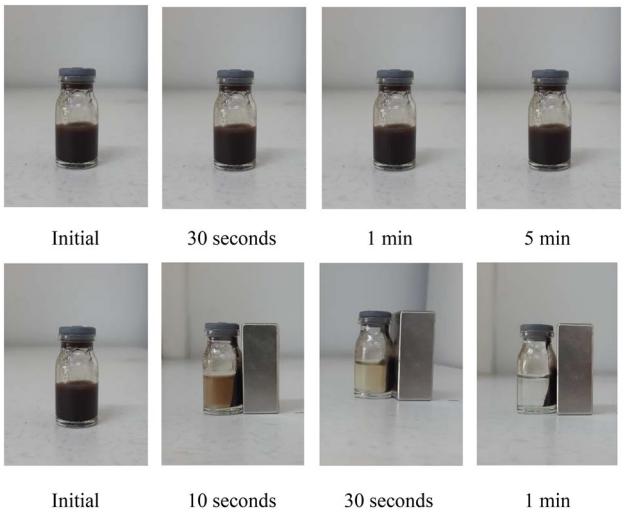

Fig. 6 Photos of magnetic separation of $Co_3O_4/Fe_3O_4@nSiO_2@mSiO_2$

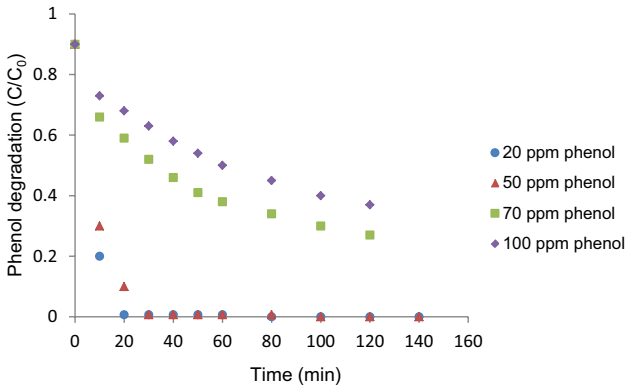

Fig. 7 Effect of phenol concentration on phenol removal. $Co_3O_4/Fe_3O_4@nSiO_2@mSiO_2$. Reaction conditions: 1 g oxone, 0.2 g catalyst, 25 ℃

medium. Therefore, it is concluded that observed color depends on the level of oxidation.

The adsorption and degradation tests on Fe_3O_4, $Fe_3O_4@nSiO_2@mSiO_2$ and $Co_3O_4/Fe_3O_4@nSiO_2@mSiO_2$ are displayed in Fig. 5. In these experiments, the Fe_3O_4 particles, support and catalyst can adsorb phenol compound at low efficiency. Adsorption performance can be seen on Fe_3O_4, $Fe_3O_4@nSiO_2@mSiO_2$, and $Co_3O_4/Fe_3O_4@nSiO_2@mSiO_2$, at 2%, 10%, and 7% in 2 h, respectively. $Fe_3O_4@nSiO_2@mSiO_2$ has much higher surface area than others, resulting in higher phenol adsorption. In oxidation procedure, the oxone without a catalyst could not oxidize phenol. Degradation process would occur when catalyst and PMS simultaneously are present in the solution. In a comparison of three material performances, $Co_3O_4/Fe_3O_4@nSiO_2@mSiO_2$ is effective in activating oxone to generate sulfate radicals. As demonstrated in the above reactions, the redox potential of M^{2+}/M^{3+} will be an important factor in generation of sulfate radical. The standard reduction potential (E°) of Co^{3+}/Co^{2+} and Fe^{3+}/Fe^{2+} is 1.92 and 0.11 V, respectively [32]. Anipsitakis and Dionysiou found that Co^{2+} and Ru^{3+} are the best transition metal catalysts for the production of freely diffusive sulfate radicals [32].

In catalytic test, the suspension is stable and homogeneous before magnetic separation. In the presence of a magnet, the particles can be separated fast. After magnet removing, particles were rapidly redispersed in solution. This shows that the catalyst possessed good water dispersion and magnetic separation (Fig. 6).

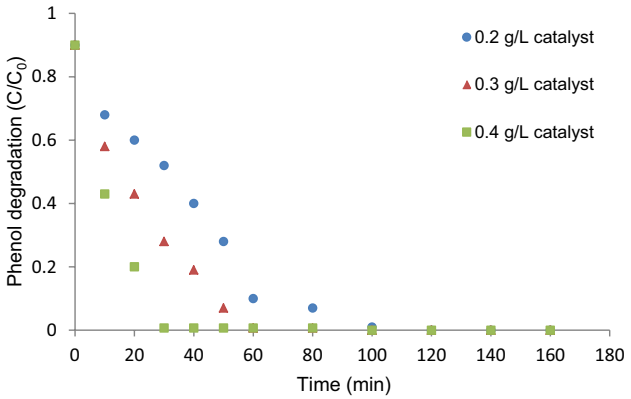

Fig. 8 Effect of catalyst loading on phenol removal. Co_3O_4/Fe_3O_4@$nSiO_2$@$mSiO_2$. Reaction conditions: 50 ppm, 1 g oxone, 25 ºC

Effects of reaction parameters on phenol degradation

All experiments were carried out in 500 mL of solution. Several parameters such as phenol concentration, catalyst loading, oxone concentration, and reaction temperature can influence phenol oxidation in solution.

Phenol concentration was the first parameter investigated in this study. Various concentrations of phenol (between 20 and 100 ppm) on the phenol oxidation are shown in Fig. 7. Overall, efficiency of phenol removal decreased with increasing phenol concentration. 100% phenol degradation could be achieved within 30 min at low phenol concentrations (20–50 ppm). At a phenol concentration of 100 ppm, efficiency of phenol removal is only 58% within 2 h.

The effect of Co_3O_4/Fe_3O_4@$nSiO_2$@$mSiO_2$ loading in solution on phenol oxidation is shown in Fig. 8. An increased amount of catalyst in the solution enhanced phenol degradation efficiency. A complete removal of phenol could be reached within 30 min at 0.4 g/L Co_3O_4/Fe_3O_4@$nSiO_2$@$mSiO_2$ loading, while with catalyst loading of 0.2 g/L, oxidation of phenol would reach 88% at 60 min.

Overall, the phenol degradation is dependent on sulfate radicals (Fig. 9). High concentration of oxidant (oxone) leads to more degradation of phenol, because oxone was the source of driving force for the forming of sulfate radicals. At 2 g/L oxone, phenol could be fully removed within 30 min. At extra oxone loading, degradation efficiency would decrease. This occurrence was possibly due to the self-quenching of hydroxyl and sulfate radicals by PMS as follows [3]:

$$OH^{\bullet} + HSO_5^- \rightarrow H_2O + SO_5^{\bullet -} \quad (7)$$

$$SO_4^{\bullet -} + HSO_5^- \rightarrow H^+ + SO_5^{\bullet -} \quad (8)$$

The reduction potential of $SO_5^{\cdot -}/HSO_5^-$ is 0.95 V at pH 7. Meanwhile, $SO_4^{\cdot -}/SO_4^{2-}$ has an oxidation potential of [2.5–3.1 V] [22].

Figure 10 reveals that reaction temperature considerably affected phenol oxidation efficiency. The formation of sulfate radicals was accelerated by increasing in temperature. Complete degradation efficiency of phenol at temperature of 25 °C would be achieved in about 30 min when the temperature was raised to 45 °C, complete removal could be achieved in about 10 min.

Adsorption of intermediates and a fraction of loose cobalt leaching from the support was caused the catalyst deactivation. In this study, the catalyst was utilized once before the regeneration by annealing in the air, using ultrasonication and washing with water. For heating treatment, after catalytic reaction, the catalysts were collected from the solution and washed with deionized water, and then, a fixed amount of catalyst was heated in 300 °C for 2 h in the presence of the air. It can remove surface-attached intermediates nearly and 100% phenol removal was achieved after 50 min. Whereas regeneration of the used catalyst using ultrasonic

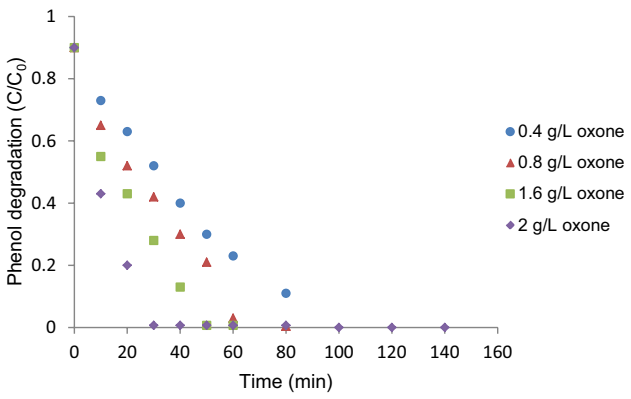

Fig. 9 Effect of oxone concentration on phenol removal. Co_3O_4/Fe_3O_4@$nSiO_2$@$mSiO_2$. Reaction conditions: 50 ppm, 0.2 g catalyst, 25 ºC

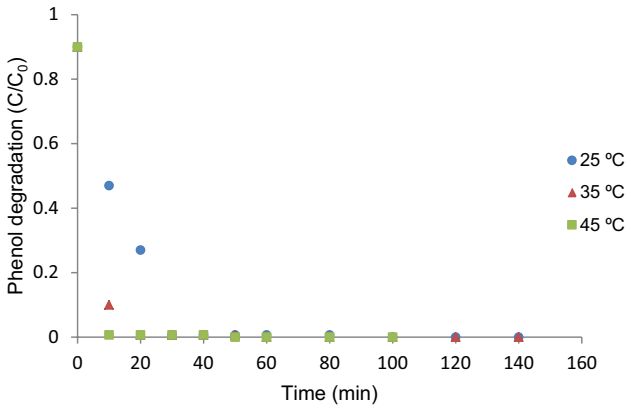

Fig. 10 Effect of temperature on phenol removal Co_3O_4/Fe_3O_4@$nSiO_2$@$mSiO_2$. Reaction conditions: 50 ppm, 1 g oxone, 0.2 g catalyst

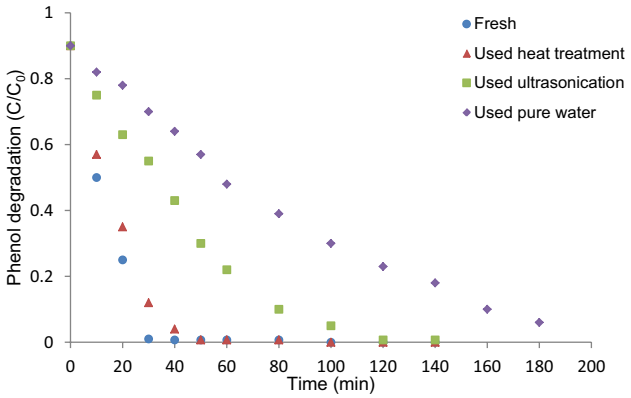

Fig. 11 Regeneration studies of the used catalyst

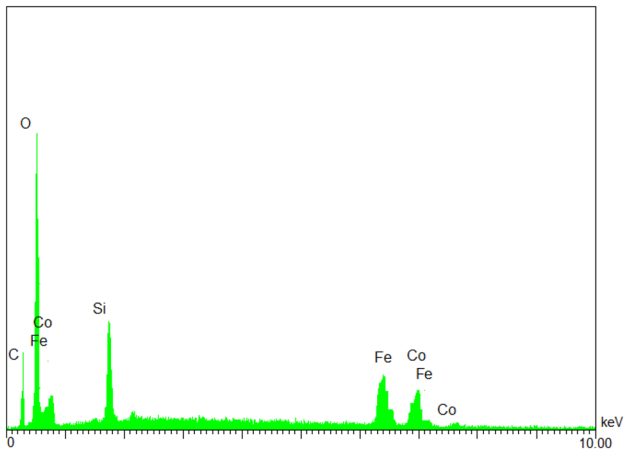

Fig. 12 EDS spectra of Co3O4/Fe3O4@nSiO2@mSiO2 after three-time use

and washing with water, partially eliminated the intermediates presented on the surface of the catalysts (Fig. 11).

The cobalt leaching was suggested to be responsible for the decreased activity in reuse. The catalyst was used three times in degradation of phenol solution. In the first time, the degradation efficiency was 100% in 30 min, in the second time, degradation efficiency was 78% in 80 min, and in the third time, degradation efficiency was 41% in 140 min. These results indicated that active phase (Co species) was separated from the surface of catalyst, therefore, degradation efficiency was decreased, and the degradation time was increased. In addition, after three-time use, the catalyst was collected from the solution and was analyzed by EDS method. This measurement illustrated that after three-time reaction, the percentage of Co was about 3 wt % (Fig. 12).

This oxidation reaction involves a reaction between cobalt and HSO_5^-, where cobalt ions are generated. These species can bind to intermediate species with hydroxyl groups substituted in benzene rings generating metal complexes. Therefore, the intermediate species can easily connect to the surface of catalyst. In addition, for evaluation of intermediates absorption on the surface of catalyst, the catalyst was collected after one-time use and washed with deionized water, and then, a fixed amount of catalyst was heated in 300 °C for 2 h in the presence of the air. By this method, apart of intermediate species can remove from the surface and 100% phenol removal was achieved after 50 min. In addition, the EDS measurement illustrated that after three-time reaction, the percentage of C and O increased that related to adsorption of intermediates' species (Fig. 12).

Conclusion

This study provides a conceivable method for employing the Fe_3O_4/silica spheres as proper support for synthesizing of based catalyst. The cobalt oxide loaded on the support was prepared by an impregnation method. Heterogeneous oxidative degradation of phenol using cobalt-supported catalyst—oxone is convenient method for waste water treatment. Efficiency of phenol oxidation is dramatically influenced by operating parameters, such as phenol and oxidant concentration, catalyst dosage, and reaction temperature. Our results illustrate that in this catalyst, oxone effectively activated; for removal of 500 mL phenol with concentration of 50 ppm, 1 gr oxone and 0.2 gr catalyst were added. Therefore, the ratio of catalyst/phenol and oxidant/phenol was equal to 8 and 40, respectively, and 100% phenol degradation occurs in 30 min. The regeneration test shows that anneals in the air could recover the catalyst activity partly. Whereas applying ultrasonic and washing with water were inappropriate regeneration methods.

Acknowledgements The authors are thankful to Research Council of Iran University of Science and Technology (Tehran) and Iran National Science Foundation (INSF) for financial support to this study.

References

1. C. St, G.M. Stoyanova, M. Georgieva, Appl. Catal., A. **208**, 243 (2001)
2. A. Fortuny. C. Bengoa., J. Font, A. Fabregat, J. Hazard. Mater. **64**, 181 (1999)

3. P. Shukla. I. Fatimah. S. Wang. H. Ang, M.O. Tadé, Catal. Today **157**, 410 (2010)
4. P. Shukla. S. Wang., K. Singh. H. Ang, M.O. Tadé, Appl. Catal., B. **99**, 163 (2010)
5. M. Anbia, M. Rezaie, Water, Air, Soil Pollut. **227**, 349 (2016)
6. M. Anbia, S. Amirmahmoodi, Scientia Iranica **18**, 446 (2011)
7. W. Liu, Chem. Res. Chin. Univ. **29**, 314 (2013)
8. S. Zarin. Z. Aslam. A. Zahir, M. S. Kamal, A.G. Rana, W. Ahmad, S. Ahmed, J. Iran. Chem. Soc. (2018) 1
9. V. Mirkhani. S. Tangestaninejad., M. Moghadam., M. Habibi, A.R. Vartooni, J. Iran. Chem. Soc. **6**, 800 (2009)
10. M. Anbia, M. Rezaie, Res. Chem. Intermediat. **43**, 245 (2017)
11. S. Wang, Dyes Pigments. **76**, 714 (2008)
12. S. Cao, K.L. Yeung, J.K. Kwan, P.M. To, C. Samuel, Appl. Catal., B. **86**, 127 (2009)
13. S. Muhammad. E. Saputra., H. Sun, S. Wang, H.-M. Ang, M.O. Tadé, Water Air Soil Pollut. **224**, 1721 (2013)
14. G.P. Anipsitakis, D.D. Dionysiou, Environ. Sci. Technol. **37**, 4790 (2003)
15. S. Yuan. Y. Fan., Y. Zhang., M. Tong, P. Liao, Environ. Sci. Technol. **45**, 8514 (2011)
16. G.P. Anipsitakis, D.D. Dionysiou, Appl. Catal., B. **54**, 155 (2004)
17. K. Chan, W. Chu, Water Res. **43**, 2513 (2009)
18. X. Chen. X. Qiao. D. Wang. J. Lin, J. Chen, Chemosphere **67**, 802 (2007)
19. J. Fernandez. P. Maruthamuthu. A. Renken, J. Kiwi, Appl. Catal., B. **49**, 207 (2004)
20. S.K. Ling. S. Wang, Y. Peng, J. Hazard. Mater. **178**, 385 (2010)
21. J. Madhavan. P. Maruthamuthu. S. Murugesan, M. Ashokkumar, Appl. Catal., A. **368**, 35 (2009)
22. P. Shukla. H. Sun. S. Wang., H.M. Ang, M.O. Tadé, Catal. Today **175**, 380 (2011)
23. E. Rahmani. A. Ahmadpour, M. Zebarjad, Chem. Eng. J. **174**, 709 (2011)
24. E. Rahmani, M. Rahmani, Green. Process. Synth. **7**, 255 (2018)
25. G.P. Anipsitakis. E. Stathatos, D.D. Dionysiou, J. Phys. Chem. B. **109**, 13052 (2005)
26. J. Barrault. M. Abdellaoui., C. Bouchoule., A. Majesté., N. Gangas, J. Tatibouet, A. Louloudi, N. Papayannakos. Appl. Catal., B. **27**, L225 (2000)
27. C.-P. Huang, Y.-H. Huang, Appl. Catal., A. **346**, 140 (2008)
28. D. Bizari. M. Rabiee., F. Moztarzadeh. M. Tahriri. S. Alavi, R. Masaeli, Ceramics–Silikáty **57**, 201 (2013)
29. Y. Kang. L. Zhou. X. Li, J. Yuan, J. Mater. Chem. **21**, 3704 (2011)
30. S. Gai. P. Yang., C. Li. W. Wang. Y. Dai. N. Niu, J. Lin, Adv. Funct. Mater. **20**, 1166 (2010)
31. H. Liang. H. Sun. A. Patel. P. Shukla. Z. Zhu, S. Wang, Appl. Catal., B. **127**, 330 (2012)
32. G.P. Anipsitakis, D.D. Dionysiou, Environ. Sci. Technol. **38**, 3705 (2004)
33. G.P. Anipsitakis., D.D. Dionysiou, M.A. Gonzalez, Environ. Sci. Technol. **40**, 1000 (2006)
34. F. Mijangos. F. Varona, N. Villota, Environ. Sci. Technol. **40**, 5538 (2006)
35. M.S. Yalfani. S. Contreras., F. Medina, J. Sueiras, Appl. Catal., B. **89**, 519 (2009)
36. L. Hu. X. Yang, S. Dang, Appl. Catal., B. **102**, 19 (2011)